A Glycosyltransferase from *Nicotiana alata* Pollen Mediates Synthesis of a Linear (1,5)-α-L-Arabinan When Expressed in Arabidopsis[1][OPEN]

Edwin R. Lampugnani, Yin Ying Ho, Isabel E. Moller[2], Poh-Ling Koh, John F. Golz, Antony Bacic, and Ed Newbigin*

Plant Cell Biology Research Centre, School of BioSciences (E.R.L., Y.Y.H., I.E.M., P.-L.K., A.B., E.N.), and School of BioSciences (J.F.G.), University of Melbourne, Melbourne, Victoria, 3010 Australia; and Australian Research Council Centre of Excellence in Plant Cell Walls, School of BioSciences, University of Melbourne, Parkville, Victoria 3010, Australia (E.R.L., Y.Y.H., I.E.M., A.B.)

ORCID IDs: 0000-0002-3666-7240 (E.R.L.); 0000-0001-9478-5459 (J.F.G.); 0000-0002-9644-302X (E.N.).

The walls of *Nicotiana alata* pollen tubes contain a linear arabinan composed of (1,5)-α-linked arabinofuranose residues. Although generally found as a side chain on the backbone of the pectic polysaccharide rhamnogalacturonan I, the arabinan in *N. alata* pollen tubes is considered free, as there is no detectable rhamnogalacturonan I in these walls. Carbohydrate-specific antibodies detected arabinan epitopes at the tip and along the shank of *N. alata* pollen tubes that are predominantly part of the primary layer of the bilayered wall. A sequence related to *ARABINAN DEFICIENT1* (*AtARAD1*), a presumed arabinan arabinosyltransferase from Arabidopsis (*Arabidopsis thaliana*), was identified by searching an *N. alata* pollen transcriptome. Transcripts for this *ARAD1*-like sequence, which we have named *N. alata ARABINAN DEFICIENT-LIKE1* (*NaARADL1*), accumulate in various tissues, most abundantly in the pollen grain and tube, and encode a protein that is a type II membrane protein with its catalytic carboxyl terminus located in the Golgi lumen. The NaARADL1 protein can form homodimers when transiently expressed in *Nicotiana benthamiana* leaves and heterodimers when coexpressed with *AtARAD1*. The expression of *NaARADL1* in Arabidopsis led to plants with more arabinan in their walls and that also exuded a guttation fluid rich in arabinan. Chemical and enzymatic characterization of the guttation fluid showed that a soluble, linear α-(1,5)-arabinan was the most abundant polymer present. These results are consistent with NaARADL1 having an arabinan (1,5)-α-arabinosyltransferase activity.

Sexual reproduction in flowering plants depends on the delivery of sperm cells to the ovule, a task that is performed by a highly specialized cell that extends from the germinated pollen grain called the pollen tube (Mascarenhas, 1993; Johnson and Preuss, 2002). Pollen tubes elongate rapidly in a strictly polar manner via the fusion of secretory vesicles, full of newly synthesized wall material, with the plasma membrane at the pollen tube tip. Reinforcing the thin primary wall laid down at the tip is a thicker, nonlignified secondary wall that is first deposited some distance behind the tip; in older pollen tubes, transverse cross walls called plugs are formed at intervals along the shank of the tube that act to separate the cytoplasmic portion of the pollen tube at the tip from spent portions of the tube closer to the grain (Ferguson et al., 1998). Although delivering the male gametes for double fertilization is the pollen tube's primary biological purpose, cell wall synthesis has been described as the pollen tube's main metabolic preoccupation because of their rapid growth rate and the diversity of locations where new cell walls appear (Heslop-Harrison, 1987).

Cell walls of *Nicotiana alata* pollen tubes grown in culture have been studied extensively, and some of the enzymes involved in their synthesis are known (Li et al., 1999; Doblin et al., 2001; Brownfield et al., 2007, 2008). The *N. alata* pollen tube wall is compositionally relatively simple compared with the primary walls of vegetative cells and contains two main polysaccharides, callose and a linear arabinan, and small amounts of cellulose, the pectic polysaccharide homogalacturonan (HG), and xyloglucan (XyG; Li et al., 1999; Lampugnani et al., 2013a). The presence of a linear arabinan in pollen tube walls is curious, as arabinan is generally found as part of the structurally complex pectic polysaccharide rhamnogalacturonan I (RG I). RG I has a backbone of

[1] This work was supported by the Australian Research Council (discovery grant no. DP110100410 to E.R.L., A.B., and E.N.) and the Centre of Excellence in Plant Cell Walls (grant no. CE1101007 to E.R.L., Y.Y.H., I.E.M., and A.B.).

[2] Present address: New Zealand Institute for Plant & Food Research Limited, Auckland 1142, New Zealand.

* Address correspondence to edwardjn@unimelb.edu.au.

The author responsible for distribution of materials integral to the findings presented in this article in accordance with the policy described in the Instructions for Authors (www.plantphysiol.org) is: Edward Newbigin (edwardjn@unimelb.edu.au).

E.R.L., A.B., and E.N. conceived and designed the experiments; E.R.L., Y.Y.H., I.E.M., P.-L.K., and J.F.G. performed the experiments; E.R.L., A.B., and E.N. wrote the article.

[OPEN] Articles can be viewed without a subscription.

www.plantphysiol.org/cgi/doi/10.1104/pp.15.02005

repeating alternating α-(1,2) rhamnose (Rha*p*) and α-(1,4) GalUA units with arabinan, a polymer of (1,5)-linked arabinofuranose residues, attached to some of the backbone Rha*p* residues (Mohnen, 2008; Atmodjo et al., 2013). Although information about function is limited, suggested roles for the arabinan branches of RG I include acting as plasticizers to confer flexibility to the wall (Jones et al., 2003), acting as mediators of cell wall hydration or cell-cell adhesion (Iwai et al., 2001; Peña and Carpita, 2004; Hansen et al., 2011; Cankar et al., 2014), and acting as a reversible link between pectin and the load-bearing cellulose network (Lin et al., 2015). However, plants can tolerate large reductions in the amount of arabinan in their walls without obvious phenotypic effects (Harholt et al., 2006). As *N. alata* pollen tube walls have no detectable Rha*p*, the arabinan in these walls is presumed to be in a free form and not part of RG I. The presence of uronic acid-free arabinans has been reported or can be inferred in other plant cell walls, either because RG I is not detectable or is present in only trace amounts or because of the behavior of arabinans in chromatographic separations (Talbott and Ray, 1992; Gibeaut et al., 2005; Cornuault et al., 2014). The function of this free class of arabinans in the wall is unknown.

Arabinan is synthesized by an arabinan (1,5)-α-arabinosyltransferase (AraT) through the transfer of an Ara residue from UDP-Ara onto an arabinan acceptor. As the Ara residues in arabinan are in the furanose form, arabinan synthesis also requires a mutase able to convert the thermodynamically favored UDP-Ara*p* form into UDP-arabinofuranose (Konishi et al., 2006, 2010). AraT activity has been observed in permeabilized membranes using both endogenous and exogenous oligosaccharide acceptors (Odzuck and Kauss, 1972; Bolwell and Northcote, 1983; Konishi et al., 2006). Additionally, genetic disruption of the Arabidopsis (*Arabidopsis thaliana*) gene *ARABINAN DEFICIENT1* (*ARAD1*) results in plants that have reduced Ara levels in their cell walls, suggesting that ARAD1 is an AraT (Harholt et al., 2006). ARAD1 is a glycosyltransferase (GT) with a type II membrane topology that belongs to the GT 47 family of the carbohydrate-active enzymes catalogued in the CAZy database (www.cazy.org; Cantarel et al., 2009). Some members of the GT 61 and GT 77 families are also AraTs, in the former case adding single arabinose residues to a xylan backbone to produce arabinoxylan and in the latter case synthesizing the short arabinosyl side chains attached to Hyp residues in glycoproteins and glycopeptides, such as extensin and CLAVATA3 (Velasquez et al., 2011; Anders et al., 2012; Xu et al., 2015).

Here, we describe the distribution of arabinan in *N. alata* pollen tube walls. Given the presence of a free arabinan in pollen tube walls, we searched an *N. alata* pollen grain transcriptome (Lampugnani et al., 2013a) for genes likely to be involved in arabinan biosynthesis. One of the putative GT complementary DNAs (cDNAs) we identified (*N. alata ARABINAN DEFICIENT-LIKE1* [*NaARADL1*]) encoded a type II membrane protein of 489 amino acids with sequence similarity to AtARAD1. Here, we show that Arabidopsis plants constitutively expressing *NaARADL1* have increased levels of arabinan in their cell walls and also produce guttation fluid in which arabinan is detected immunologically. Subsequent enzyme digestions and electrospray ionization-tandem mass spectrometry (ESI-MS^2) analysis confirmed the presence of a linear (1,5)-α-L-arabinan in the guttation fluid. The results are consistent with NaARADL1 having AraT activity.

RESULTS

Distribution of Arabinan in *N. alata* Pollen Tubes

The distribution of arabinan epitopes in *N. alata* pollen tubes grown in culture for either 4 or 16 h was examined with monoclonal antibodies LM6 and LM13 (Fig. 1). LM6 binds to a (1,5)-α-L-oligoarabinoside of between five and six residues (Willats et al., 1998), whereas LM13 recognizes a longer, linear arabinan epitope (Verhertbruggen et al., 2009). After 4 h of growth, LM6 labeling was evenly distributed along the entire pollen tube, including the tube tip (Fig. 1, A and B). LM13 labeling was also distributed along the entire shank of the pollen tube and at the tube tip, but its distribution was notably patchier (Fig. 1, C and D). After 16 h of growth, LM6 labeling remained unchanged (Fig. 1, E and F), whereas LM13 labeling was now absent from the shank of the pollen tube but was still present at the tip (Fig. 1, G and H). An immunogold transmission electron micrograph of LM13 labeling in a 4-h pollen tube shows that the longer arabinan epitope was deposited predominantly in the thin outer fibrillar primary wall of the bilayered tube wall (Fig. 1I).

Characterization of a Putative Arabinanosyl Transferase from *N. alata* Pollen

Searching the *N. alata* pollen grain transcriptome identified a contig with 38% amino acid identity to AtARAD1 (Supplemental Fig. S1). The full-length sequence amplified from pollen grain cDNA was predicted to encode a protein with a single transmembrane domain belonging to CAZy family GT 47 (www.cazy.org) that was likely targeted to the Golgi apparatus and inserted into the membrane in a type II orientation. This protein was named NaARADL1, as its closest Arabidopsis ortholog is the uncharacterized ARAD1-related protein encoded by At3g45400 (Fig. 2). Consistent with this not being the *N. alata* AtARAD1 ortholog, sequencing of the *NaARADL1* gene revealed that it had two exons and a single 1,338-bp intron, the same organization as At3g45400 and a different organization from *AtARAD1*, which has three exons and two introns (Supplemental Fig. S2).

To better understand the relationships between the putative NaARADL1 and likely orthologs in other plant species, a phylogenetic tree was constructed of the GT 47 subclade that includes AtARAD1. Li et al. (2004)

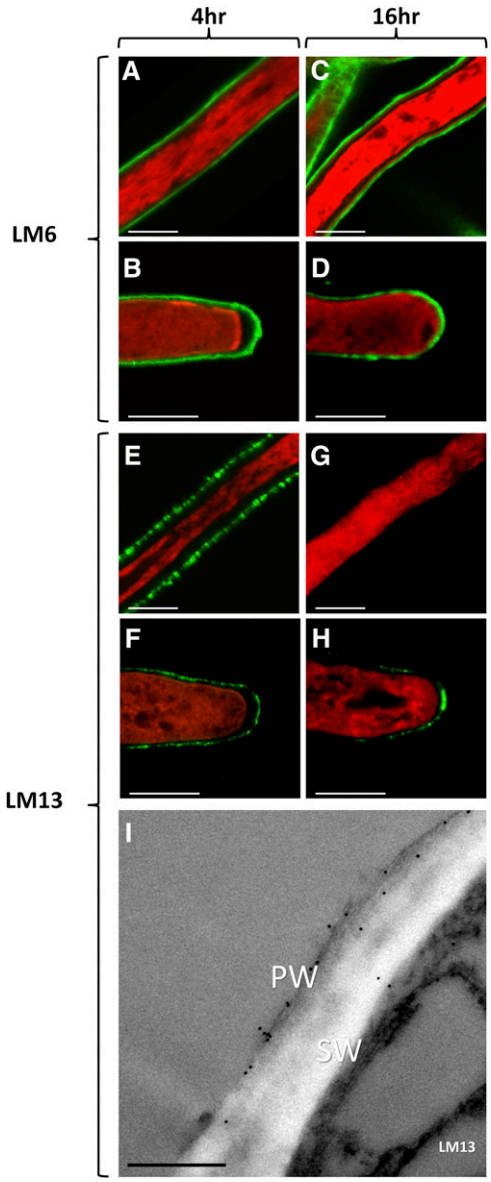

Figure 1. Distribution of arabinan in the walls of *N. alata* pollen tubes grown in vitro. Arabinan epitopes were detected (green) with the monoclonal antibodies LM6 and LM13. Pollen tubes were counterstained with FM4-64 (red). A to D show 4-h (A and B) and 16-h (C and D) pollen tube shank (A and C) and tip (B and D) regions labeled with LM6. E to H show 4-h (E and F) and 16-h (G and H) pollen tube shank (E and G) and tip (F and H) regions labeled with LM13. I shows a cross section of a 4-h pollen tube shank imaged with immunogold transmission electron microscopy labeled with the monoclonal antibody LM13. PW, Fibrillar primary wall; SW, electron-lucent secondary wall. Bars = 5 μm.

previously classified the GT 47 family into six separate subclades (A–F), with AtARAD1 belonging to subclade B. Figure 2 shows a maximum likelihood tree of GT 47 subclade B proteins from selected flowering and nonflowering plants with fully sequenced genomes: the eudicots Arabidopsis, potato (*Solanum tuberosum*), and tomato (*Solanum lycopersicum*), the grasses maize (*Zea mays*) and rice (*Oryza sativa*), the spikemoss *Selaginella moellendorffii*, and the moss *Physcomitrella patens*. *NaARADL1* belongs to a well-resolved cluster of flowering plant sequences that also included At3g45400 and two *Solanum* spp. proteins. This cluster was separate from the larger AtARAD1-containing cluster.

Reverse transcription-PCR analysis confirmed *NaARADL1* expression in pollen grains and growing pollen tubes as well as various vegetative tissues (Supplemental Fig. S3). Our attempts to better define *NaARADL1* expression using RNA in situ hybridization were unsuccessful because the low level of expression meant that signal could not be distinguished from background in vegetative and floral tissues (Supplemental Fig. S4). Instead, expression was studied in Arabidopsis using a GUS reporter construct that included the sequence 2.3 kb upstream of the *NaARADL1* coding region (pNaARADL1:GUS; Fig. 3). As well as the expected strong GUS activity in anthers, GUS activity was detected in root (Fig. 3A) and shoot apices (Fig. 3B), in developing and fully expanded leaves and leaf axils (Fig. 3, C–F), and in developing ovules (Fig. 3G). GUS activity also was seen in growing pollen tubes (Fig. 3I) and in nectaries (Fig. 3J).

NaARADL1 Is a Type II Golgi Protein Able to Form Homodimers and Heterodimers

The subcellular location of NaARADL1 was determined using fluorescently tagged proteins and transient expression in *N. alata* pollen and *Nicotiana benthamiana* leaves. In both instances, the fluorescent reporter was translationally fused to the C terminus of NaARADL1 (NaARADL1-CERULEAN in pollen and NaARADL1-VENUS in leaves). In growing *N. alata* pollen tubes, NaARADL1-CERULEAN fluorescence was associated with numerous highly motile organelles that were distributed throughout the cytosol and excluded from the clear zone at the tip (Fig. 4, A–D; Supplemental Movie S1). The movement of these organelles showed a bidirectional streaming pattern typical of actively growing pollen tubes. In *N. benthamiana* leaves, NaARADL1-VENUS produced a punctate fluorescence pattern that was associated with Golgi-located proteins (Fig. 3E). Supporting a Golgi location, NaARADL1 colocated with the Golgi marker SIALYLTRANSFERASE in pollen tubes (Fig. 4, B–D) and α-MANNOSIDASE I in leaves (Fig. 4, F–H). The subcellular location of NaARADL1 did not overlap with that of the endoplasmic reticulum marker SP-WAK2-mCERULEAN-HDEL in *N. benthamiana* leaves (Fig. 4, E and G).

NaARADL1 is predicted to be a type II membrane protein with the N terminus on the cytoplasmic side of the membrane and the C-terminal catalytic end within the Golgi lumen. To confirm this membrane topology, we used the GO-PROMTO bimolecular fluorescence complementation (BiFC) assay (Søgaard et al., 2010) and transiently expressed combinations of constructs with either cytosolic or lumenal fluorescent reporters in *N. benthamiana* leaves. The combinations that were

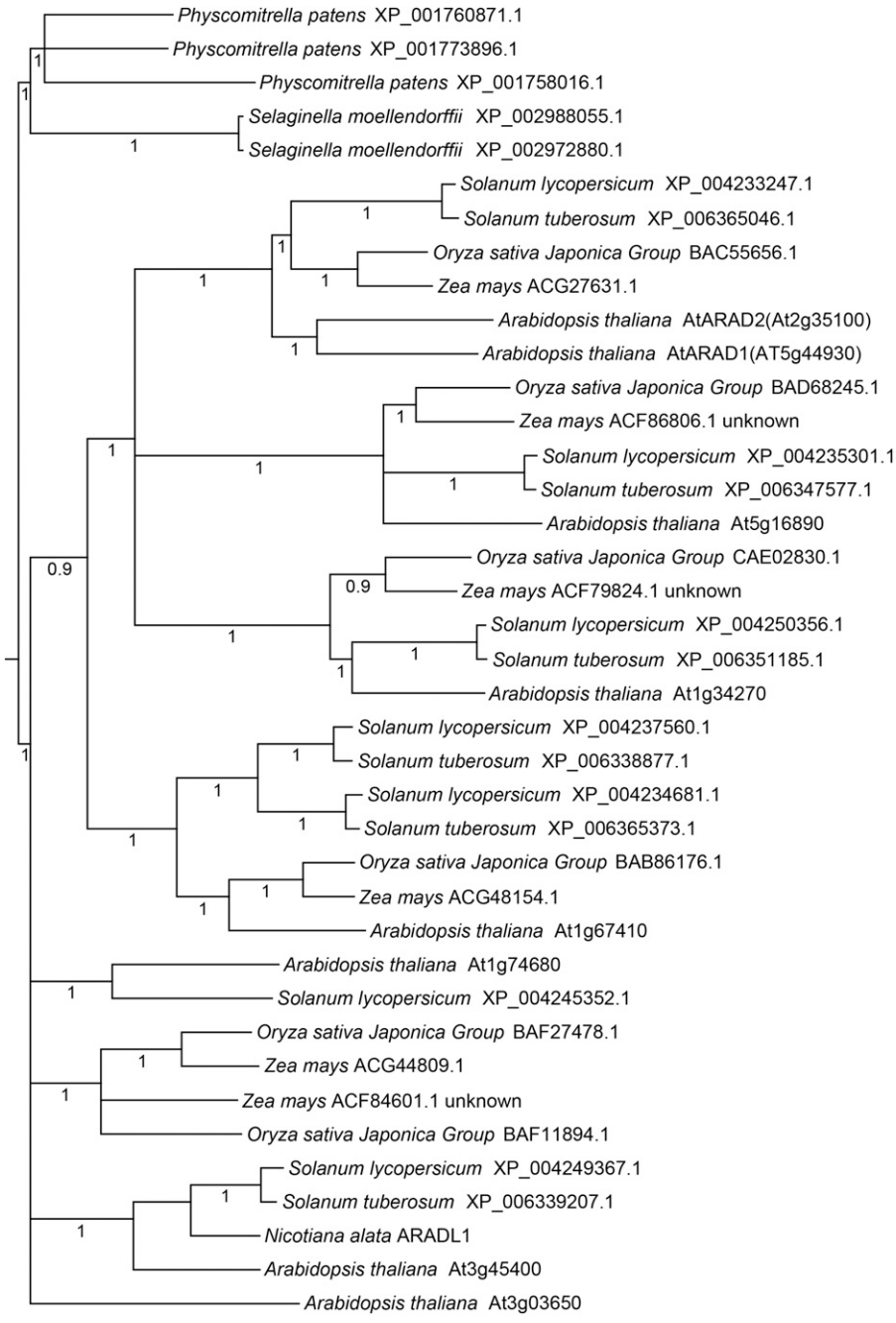

Figure 2. Phylogenetic tree of GT 47 subclade B from selected flowering and nonflowering plants. The phylogenetic tree shows relationships among 38 AtARAD1-like protein sequences from representative bryophytes (*P. patens*), lycopods (*S. moellendorffii*), and angiosperms (rice, maize, tomato, potato, and Arabidopsis) and the *N. alata* sequence NaARADL1. Numbers indicate Bayesian posterior probability support for the node. Less supported nodes (posterior probability < 0.9) have been collapsed.

transiently coexpressed included the test constructs NaARADL1-VN and NaARADL1-VC, in which amino acids 1 to 155 or 155 to 240 of VENUS are attached to the C-terminal end of NaARADL1, and the luminal (VN-TMD and VC-TMD) and cytosolic (TMD-VN and TMD-VC) reporter constructs. The only test/reporter pairs that consistently elicited a fluorescent signal were those that included a luminal reporter and its complementary NaARADL1 test construct (Fig. 5). These results indicate that the C-terminal catalytic domain of NaARADL1 is in the Golgi lumen and that NaARADL1 adopts a type II membrane protein topology.

The Arabidopsis protein AtARAD1 forms homodimers and is capable of forming heterodimers with the related protein AtARAD2 (Harholt et al., 2012). To test if NaARADL1 is also capable of forming homodimers in planta, interactions between the NaARADL1-VN and NaARADL1-VC test constructs were assessed by BiFC. For these experiments, homodimerization of the Golgi-localized galactosyltransferase MUR3 was used as a positive control (Madson et al., 2003). As expected, coexpression of the complementary constructs MUR3-VN and MUR3-VC produced punctate fluorescence in the Golgi (Fig. 6A), whereas no fluorescence was

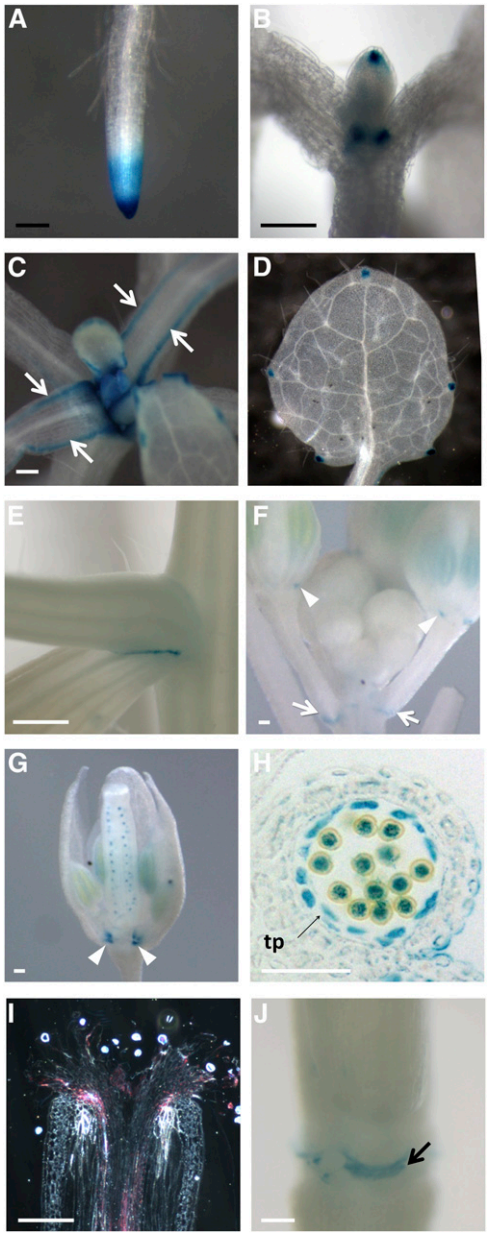

Figure 3. Histochemical staining of pNaARADL1:GUS-expressing Arabidopsis plants. Seedlings 7 d after germination (DAG) show GUS staining in roots, particularly at the root tip (A), and the tip of the developing leaf and its basal organ boundary (B). Seedlings 14 DAG show GUS activity along the margins of the leaves (arrows; C). In fully expanded leaves, GUS accumulation is limited to the hydathodes (D). GUS also accumulates between the axils of secondary shoots (E), at the junction of the pedicel with the stem (arrows; F), and at the base of the sepals in the intersepal zone (arrowheads; F and G). Expression is also evident in the developing ovules (G) and developing anther (I), including the tapetum (tp), pollen grains, and pollen tubes growing through the style, as viewed in a longitudinal section under dark-field optics. Expression is also present in the nectaries (J). Black bars = 1 mm; white bars = 250 μm.

detectable when MUR3-VN and NaARADL1-VC or NaARADL1-VN and MUR3-VC were coexpressed in leaves (Fig. 6, B and C). In contrast, coexpression of NaARADL1-VN and NaARADL1-VC produced strong fluorescence in a pattern consistent with a Golgi location, indicating that NaARADL1 forms homodimers (Fig. 6D). The ability of NaARADL1 and AtARAD1 to interact in planta was also tested by coexpressing AtARAD1-VN and AtARAD1-VC. First, we confirmed that coexpressing complementary AtARAD1 constructs results in the production of a fluorescent signal due to homodimerization (Fig. 6G). We then tested for heterodimerization by coexpressing either NaARADL1-VN and AtARAD1-VC or AtARAD1-VN and NaARADL1-VC (Fig. 6, H and I). In both cases, a positive fluorescent signal was detected with the pattern of fluorescence consistent with a Golgi location.

Arabidopsis Plants Expressing NaARADL1 Have Increased Levels of (1,5)-α-Arabinan

To further test whether NaARADL1 has arabinosyltransferase activity, *NaARADL1* was expressed in Arabidopsis plants under the control of the strong constitutive cauliflower mosaic virus 35S promoter. To identify T1 plants with high-level expression, NaARADL1 was C-terminally fused to the fluorescent protein VENUS. Homozygous lines were generated from the four most strongly fluorescent T1 plants, and walls (as an alcohol-insoluble residue) were prepared 20 DAG and subjected to linkage analysis by methylation (Supplemental Table S1). Linkage analyses identified a 30% increase in 1,5-Ara(*f*) (the main residue type in arabinan) in the walls of the *NaARADL1*-expressing lines compared with Columbia-0 (Col-0; $P < 0.05$), but no change in either the 1,2,5-Ara(*f*) arabinan branch points or in terminal Ara. Although amounts were low, transgenic plant lines also had more substituted Rha [1,2,4-Rha(*p*)] than Col-0 (Supplemental Table S2). However, as the ratio of unsubstituted 1,2-Rha(*p*) to substituted Rha(*p*) [1,2,4-Rha(*p*)] in the transgenic lines (1:2.3) was roughly similar to that in Col-0 (1:2.5), there appeared to be no change in the number of side chains attached to RG I. Thus, a similar number of arabinan side chains was attached to the RG I in the NaARADL1-expressing lines, but the length of arabinan side chains was apparently longer.

Although the overall growth phenotype of *NaARADL1*-expressing lines was similar to that of the wild type, these plants often accumulated droplets of a clear fluid at the base of their rosette leaves, a phenotype never observed in wild-type plants grown under the same conditions (Supplemental Fig. S5). To determine if the exudate was a guttation fluid, root xylem sap was collected from decapitated stumps of wild-type and transgenic plants. The xylem sap flow of transgenic plants (2.1 ± 0.04 μL mg^{-1} h^{-1}; $n = 10$) was almost 4 times that of wild-type controls (0.54 ± 0.06 μL mg^{-1} h^{-1}; $n = 10$, $P < 0.001$), consistent with increased root pressure causing the excretion of guttation fluid from leaf hydathodes of *NaARADL1*-expressing plants.

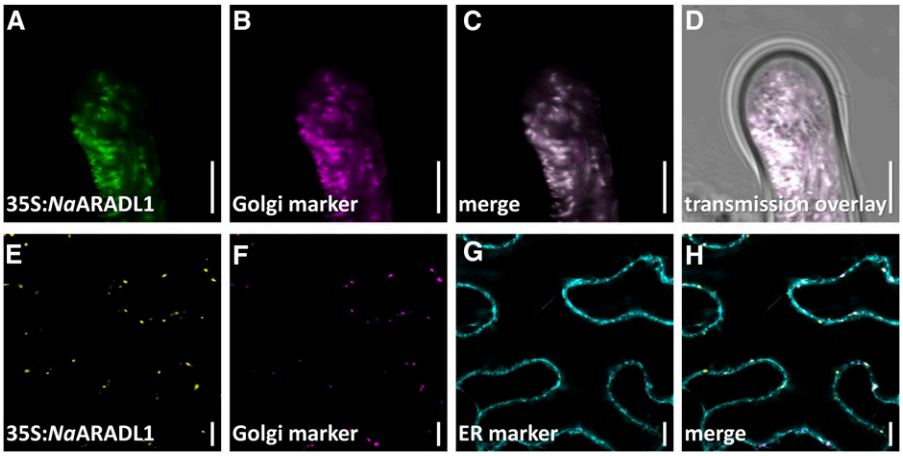

Figure 4. Subcellular locations of fluorescently tagged versions of NaARADL1 in transiently transformed *N. alata* pollen tubes (A–D) and *N. benthamiana* leaves (E–H). A to D, Imaging of *N. alata* pollen grains transiently cotransformed with pLAT52:NaARADL1-CERULEAN (green) and the Golgi marker rat sialyltransferase translationally fused to dsRED (magenta). The merged and bright-field images of this cell also are shown. E to H, Imaging of *N. benthamiana* leaf cotransformed with the NaARADL1-VENUS translational fusion (yellow), the mCHERRY fluorescent Golgi apparatus marker soybean α-(1,2)-MANNOSIDASE I (magneta), and the endoplasmic reticulum (ER) marker SP-WAK2-mCERULEAN-HDEL (cyan). The merged image is also shown. Bars = 10 μm.

To determine whether cell wall-associated polysaccharides and proteoglycans were present in the exudate, wild-type and *NaARADL1*-expressing plants were grown overnight under high humidity to promote guttation. The guttation fluid was collected and analyzed by comprehensive microarray polymer profiling (CoMPP; Moller et al., 2012) using antibodies that detect epitopes associated with arabinan, XyG, HG, heteroxylans, and arabinogalactan proteins (AGPs). While none of the tested epitopes were present in guttation fluid collected from wild-type plants, guttation fluid from all six independent transgenic *NaARADL1*-overexpressing lines contained arabinan epitopes (Supplemental Fig. S6). The guttation fluid from these plants contained HG and AGP, with most lines also secreting low but detectable levels of XyG.

Although the guttation fluid of *NaARADL1*-expressing plants contained detectable polysaccharide, the carbohydrate concentration of the fluid was low (9.66 ng μL^{-1}; Table I). Methanolysis detected only four monosaccharides in the guttation fluid: Ara, Xyl, Gal, and Glc. Neither Rha nor GalA was detected. Of the four monosaccharides, Ara was the most abundant, at about 57% of the total; most of the Ara was in a polymeric form (94.6%). Methanolysis results thus were consistent with CoMPP analysis and suggested the *NaARADL1*-expressing plants excrete an arabinan-rich guttation fluid.

The fine structure of the arabinan was determined by digesting the guttation fluid with an endo-α-(1,5)-arabinase, and after methylation, the released oligosaccharides were analyzed by matrix-assisted laser desorption-time of flight-mass spectrometry (MALDI-TOF-MS) and ESI-MS^2. Sugar beet (*Beta vulgaris*) arabinan was used as a control. MALDI-TOF-MS of the sugar beet arabinan revealed a series of oligosaccharides (mass-to-charge ratio [*m/z*] 1,351.009, 1,190.545, 1,029.686, and 869.914) that were diagnostic of a pentose series from degree of polymerization (DP) 5 to DP8 (Fig. 7A). A similar pentose series also was seen in the guttation fluid with two quasi-molecular ions of *m/z* 869.792 and 1,029.965, corresponding to DP5 and DP6 oligosaccharides, predominating (Fig. 7B). The sequence of the pentose series was verified by ESI-MS^2 fragmentation of the sodiated quasi-molecular ion at *m/z* 1,029 (DP6) from the guttation fluid (Supplemental Fig. S7A). Fragmentation of glycosidic bonds from the non-reducing-end residue generated Y-series fragment ions of *m/z* 855, 695, 535, 375, and 215 that were separated by *m/z* 160 (methylated pentose). In addition, ring fragmentation cleavage produces X-series ions diagnostic of the linkages between adjacent glycosyl residues (Domon and Costello, 1988). In this case, the sodiated ion *m/z* 271 was diagnostic of ring fragmentation in reducing-end pentoses joined by either a 1,4- or 1,5-linkage (Supplemental Fig. S7B). These multi-stage mass spectrometry data, when combined with the linkage analysis (Supplemental Table S2), where 1,5-Ara(*f*) is the predominant Ara linked residue, confirm that these are oligo-(1,5)-α-arabinofuranosides.

In summary, the compositional analyses (monosaccharide/tandem mass spectrometry/enzymic/CoMPP) confirm that the predominant polysaccharide in the guttation fluid of *NaARADL1*-expressing lines was a soluble α-(1-5)-L-arabinan. Taken together, the results suggest that NaARADL1 is an AraT.

DISCUSSION

This article describes the distribution of arabinan in *N. alata* pollen tubes and identifies the Golgi-located

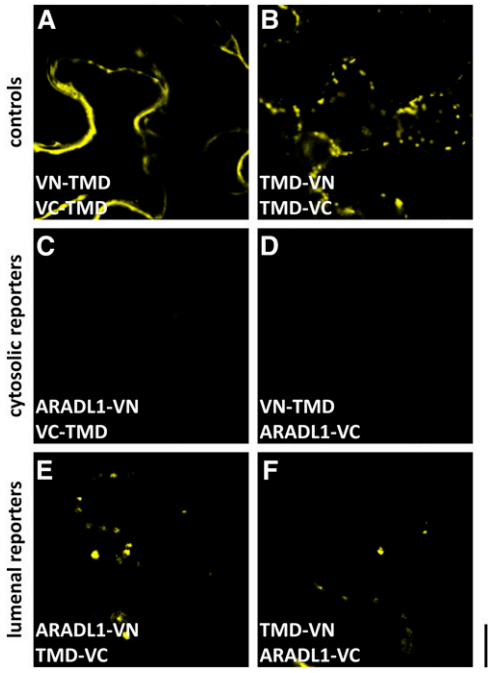

Figure 5. GO-PROMTO analysis showing that NaARADL1 is a type II membrane protein located in the Golgi apparatus. A and B, Coexpression of either the cytosolic reporters VN/VC-TMD (A) or the luminal Golgi apparatus reporters TMD-VN/VC (B). C and D, No fluorescence was detected when NaARADL1-VN or NaARADL1-VC was coexpressed with the cytosolic reporters VC-TMD (C) or VN-TMD (D). E and F, A positive signal was detected when either NaARADL1-VN or NaARADL1-VC was coexpressed with the Golgi apparatus luminal reporter TMD-VC (E) or TMD-VN (F), indicating that the C terminus of NaARADL1 is located in the lumen. Bar = 10 μm.

protein NaARADL1 as mediating its synthesis. Arabinans are generally thought of as a component of RG I, although the walls of *N. alata* pollen grains and tubes lack detectable Rha(*p*), suggesting that RG I is not in these cell walls (Li et al., 1999; Lampugnani et al., 2013a). Additionally, in the Solanaceae, Ara also can be attached to XyG as single Ara residues or short oligosaccharides to make an arabinosylated form called arabinoxyloglucan (Sims et al., 1996; York et al., 1996). However, in *N. alata* pollen grains and tubes, the XyG is fucosylated and no arabinoxyloglucan is detectable (Lampugnani et al., 2013a; Dardelle et al., 2015). Thus, we consider the arabinan in *N. alata* pollen tube walls to be in a free form, with free here meaning that it is not associated with RG I. The arabinan in *N. alata* pollen tubes, however, could still form part of some other wall polysaccharide; indeed, it could conceivably be attached to more than one polysaccharide. In pollen tube walls of species like Arabidopsis, levels of Rha(*p*) are such that RG I is very likely present (Dardelle et al., 2010). But it should be noted that even in some RG I-containing vegetative cell walls, it has been suggested that up to 60% of the arabinan can exist in a uronic acid-free, hemicellulosic form (Talbott and Ray, 1992). It thus seems plausible for the free arabinan described here in *N. alata* pollen tubes to be a component of other plant cell walls as well. Consistent with this, *NaARADL1* is expressed not only in pollen grains and tubes but in a variety of vegetative tissues as well, with promoter::GUS analysis in Arabidopsis pointing to expression in meristematic tissues, secretory cells like nectaries, and during male and female reproductive development (Fig. 3).

NaARADL1 belongs to the CAZy GT 47 family, a major family of nonprocessive, inverting-type GTs (Geshi et al., 2011). In addition to members with putative AraT activity, this family includes enzymes capable of transferring at least three different types of donor sugars, Xyl, Gal, and GlcA residues, to various cell wall polysaccharides, both pectins and cross-linking noncellulosic polysaccharides (Zhong et al., 2005; Brown et al., 2009; Wu et al., 2009). Within the GT 47 family, NaARADL1 and the two putative Arabidopsis AraTs, AtARAD1 and AtARAD2 (Harholt et al., 2006, 2012), are part of subclade B (Fig. 2). Phylogenetic reconstruction of the GTs in this subclade using sequences from eudicots, grasses, fern allies, and mosses shows broad taxonomic clustering, with the *Selaginella* and *Physcomitrella* spp. GTs grouping together in a separate cluster from the angiosperm sequences. Within the angiosperms, there are several well-supported clades, with most clades containing both eudicot (Arabidopsis and *Solanum* spp.) and grass (rice and maize) representatives. This suggests that these lineages were established early in the diversification of flowering plants and that the B subclade contains GTs with a diverse range of functions. Subfunctionalization within subclade B is evident even within a lineage, as the two characterized Arabidopsis GTs, AtARAD1 and AtARAD2, represent a recent duplication but are nonredundant enzymes, as expression of AtARAD2 cannot rescue the reduced arabinan levels seen in *arad1* mutants (Harholt et al., 2012). NaARADL1 and its Arabidopsis ortholog, the uncharacterized protein encoded by At3g45400, are in a separate lineage from the ARAD proteins. This lineage contains the Arabidopsis gene At3g03650, also known as *EMBRYO SAC DEVELOPMENT ARREST5/TUBE GROWTH DEFECTIVE5* (*EDA5/TGD5*; Pagnussat et al., 2005; Boavida et al., 2009). Genetic disruption of *EDA5/TGD5* results in defects in pollen tube elongation and in the embryo sac at an early stage of development.

Previous work with the Arabidopsis mutant *arad1* found that similar numbers of arabinan side chains were attached to RG I but that the chains were smaller, suggesting that AtARAD1 is involved in chain elongation (Harholt et al., 2006, 2012). However, despite *AtARAD1* expression complementing the *arad1* mutant phenotype, none of the transformed plants had more arabinan than the wild-type level and arabinan levels were not increased when *AtARAD1* was expressed in a wild-type background. Reasons advanced to explain why arabinan levels were not higher included a limiting supply of nucleotide sugar substrates and the availability of interacting proteins (Harholt et al., 2006). As a 30% increase in arabinan levels was seen in

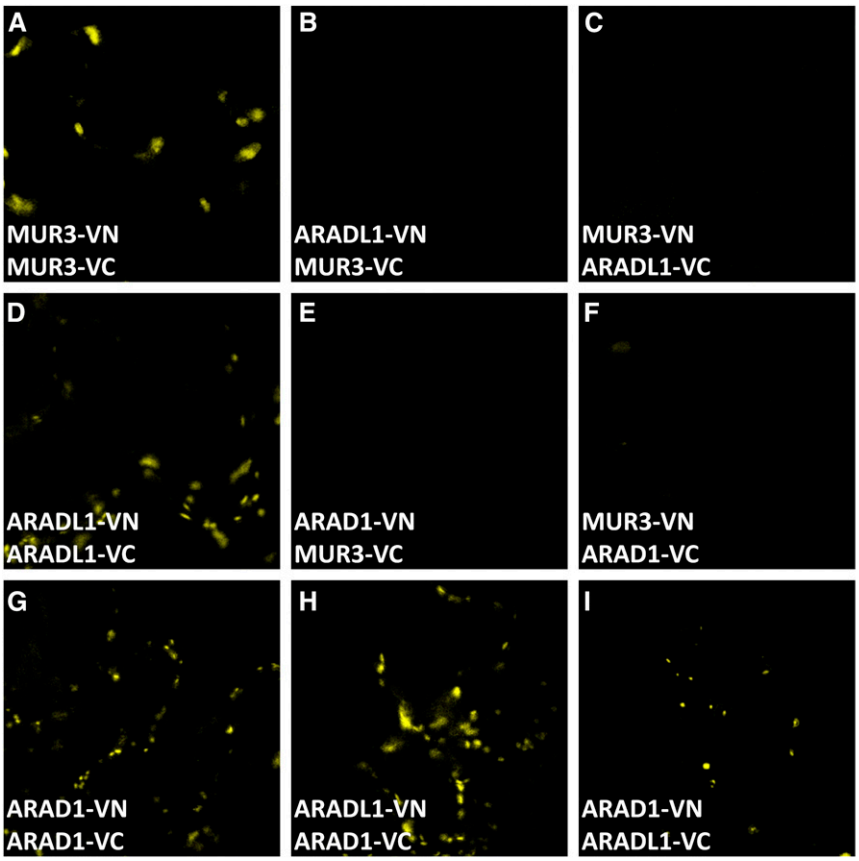

Figure 6. BiFC analysis showing that NaARADL1 forms homodimers and can heterodimerize with AtARAD1. A, Coexpression of the C-terminal VN or VC fusions of NaMUR3. B to D, Expression of NaARADL1-VN and NaMUR3-VC (B), NaMUR3-VN and NaARADL1-VC (C), or NaARADL1-VN and NaARADL1-VC (D). E and F, Negative controls including AtARAD1-VN/VC (E) and NaMUR3-VC/VN (F). G to I, Coexpression of AtARAD1-VN and AtARAD1-VC (G) or NaARADL1-VN/VC with AtARAD1-VC/VN (H and I). Bar = 10 μm.

NaARADL1-overexpressing Arabidopsis lines, in this instance it appears that neither nucleotide sugar substrates nor interacting proteins were limiting. Possibly, AtARAD1 is not responsible for arabinan chain elongation but instead attaches the first or one of the early Ara residues to the RG I backbone (Geshi et al., 2011). Based on this scenario, NaARADL1 would be an arabinan (1,5)-α-AraT that uses linear arabino-oligosaccharides as acceptors, an activity that is consistent with its presumed function in *N. alata* pollen tubes.

However, other possible explanations exist. For example, NaARADL1 could be part of a protein complex that synthesizes arabinan but helps stabilize this complex rather than acting as its catalytic component. In this scenario, increased arabinan levels in the overexpressing lines are not due to NaARADL1's inherent catalytic activity but to an increase in complex stability. Homogalacturonan synthesis provides a relevant instance of this, as the related GTs GAUT1 and GAUT7 are part of the HG-synthesizing complex, with GAUT1 directly responsible for biosynthesis and GAUT7 for anchoring the complex into the Golgi membrane (Atmodjo et al., 2011). Consistent with an auxiliary function in arabinan synthesis is NaARADL1's ability to form heterodimers with related GT 47s such as AtARAD1. Ultimately resolving these alternatives requires an assay for arabinan arabinosyltransferase activity that uses heterologously expressed proteins. Although a suitable assay exists (Konishi et al., 2006), attempts so far to detect activity using recombinant AtARAD1 and AtARAD2 have been unsuccessful (Harholt et al., 2012).

Table I. *Monosaccharide composition analysis of guttation fluid collected from plants expressing 35S:NaARADL1-VENUS*

	Neutral Sugar[a]			
	Ara	Xyl	Gal	Glc
Exudate	57.2 ± 1.13 (51.8[b])	3.5 ± 0.16	18.2 ± 1.27	21.2 ± 2.23 (12.7[b])

[a]Values shown are percentages of peak area relative to total peak areas, determined by methanolysis and gas chromatography-mass spectrometry carried out on two biological replicates with two technical replicates each. [b]The percentage of monosaccharide that is part of a polymer (i.e. corrected for free monosaccharide in the guttation fluid).

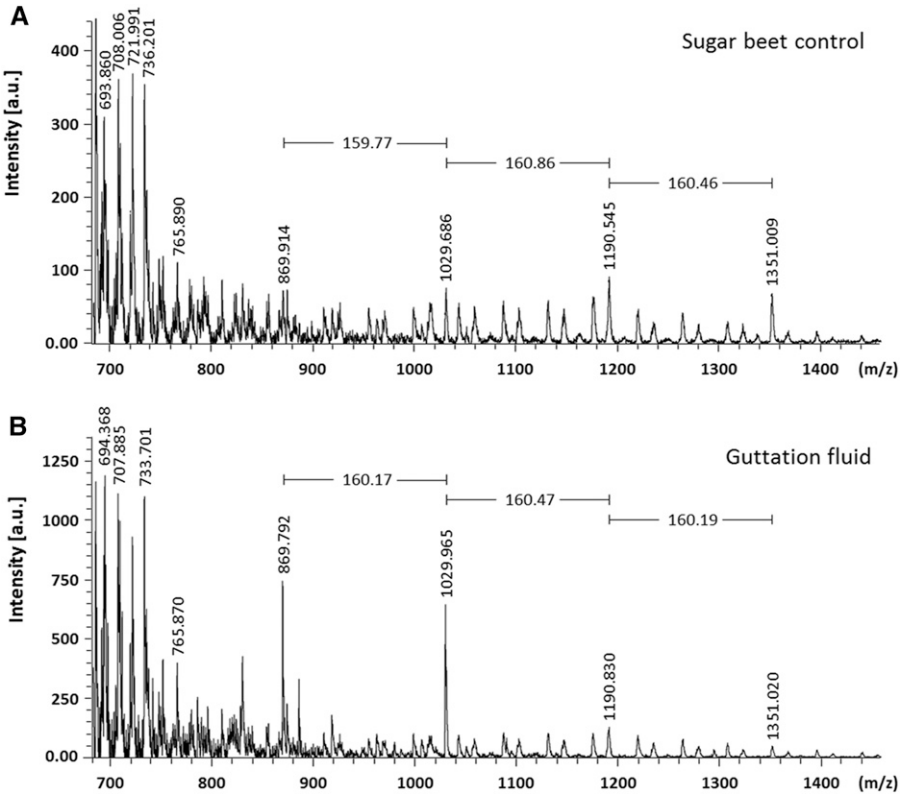

Figure 7. MALDI-TOF-MS analysis of endoarabinase-digested guttation fluid from plants expressing 35S:NaARADL1-VENUS. Endoarabinase generated arabinosyl oligosaccharides released from the sugar beet control (A) and guttation fluid collected from 35S:NaARADL1-VENUS-expressing plants (B). a.u., Arbitrary units.

In addition to the increase in cell wall arabinan, *NaARADL1*-expressing lines also secreted an arabinan-rich guttation fluid. Since methanolysis showed that the guttation fluid contained no Rha, the arabinan can be considered free. However, it is important to note that the arabinan was unlikely to exist in the guttation fluid as free low-M_r oligosaccharides, as no major peaks were evident in the MALDI-TOF-MS spectra of the permethylated and undigested guttation fluid up to approximately DP40 to DP50. In addition, linear arabinans are poorly soluble in aqueous solutions, and their ability to form hazes in fruit juices and red wine is well known (Churms et al., 1983; Beveridge and Wrolstad, 1995). More likely, the arabinan was linked to a highly soluble branched polysaccharide(s), although the identity of this polysaccharide is unknown. However, CoMPP analysis showed the presence of variable amounts of other cell wall polysaccharides and proteoglycans in the guttation fluid, including HG, AGPs, and trace amounts of XyG.

Two questions arise from the presence of a linear arabinan in the guttation fluid. How does this polysaccharide enter the guttation fluid? And why do plants expressing *NaARADL1* release such a fluid?

During guttation, water and solutes from the xylem exit the leaf through natural openings on the leaf margins called hydathodes (Esau, 1977). One of the functions of guttation is to relieve root pressure, the hydrostatic pressure caused when roots take up excessive amounts of water because the water potential of xylem sap is more negative than that of the surrounding soil (Takeda et al., 1991; Wegner, 2014). The higher rates of xylem sap flow observed in the transgenic plants were consistent with increased root pressure causing the production of a guttation fluid. Although transport into xylem is apoplastic and requires solutes to be loaded into xylem vessels and tracheid conducting cells, the Casparian strip prevents apoplastic transport into the stele itself from cell layers outside the endodermis. Solutes entering the xylem instead must be transported symplastically in a process that requires two transmembrane transport events: import into either a cortical or epidermal cell and export from either the pericycle or a xylem parenchyma cell (Turnbull and Lopez-Cobollo, 2013). As there are no transporters in plants able to transport wall polysaccharides in this manner, it is most likely that the arabinan in guttation fluid is derived from cells in the stele itself. These cells presumably shed the arabinan-containing material, which is then loaded directly into the xylem from the stelar apoplastic space. The presence of soluble polysaccharides in the xylem sap would reduce the water potential, causing more water to enter the root with the increase in root pressure, consequently leading to guttation.

In conclusion we have shown that NaARADL1 is a type II Golgi protein belonging to subclade B of the diverse CAZy GT 47 family. NaARADL1 most likely has arabinan (1,5)-α-AraT activity that is able to extend arabinan chains, although it also may function in some other way to facilitate arabinan synthesis, for instance

as a complex-stabilizing auxiliary protein. In *N. alata* pollen tubes, NaARADL1 mediates the synthesis of the free arabinan found in the cell wall and, when expressed in Arabidopsis, mediates the synthesis of an arabinan that is most likely attached to RG I as well as a free arabinan that is part of an unknown but soluble polysaccharide(s) shed by cells into the apoplastic space. NaARADL1 may elongate each of these acceptors by acting either as a homodimer or in a multifunctional way by associating with endogenous Arabidopsis AraTs to form various heterodimers. Much of the work done to date on arabinan and its function has relied on the use of antibodies to detect arabinan epitopes in cell walls (Verhertbruggen et al., 2009, 2013; Cornuault et al., 2014). Given the diversity of arabinan structures in the wall and their highly dynamic nature, there is a need for further research to better define arabinans, especially the understudied free type, to describe the functions of each arabinan type in muro and to understand how the GT 47s from subclade B interact to direct their synthesis.

MATERIALS AND METHODS

Plant Materials

Plants were grown in soil in a glasshouse either with continuous cool-white fluorescent lights and natural daylight at 20°C to 26°C (for Arabidopsis [*Arabidopsis thaliana*] and *Nicotiana benthamiana*) or under natural daylight at 23°C to 30°C (for *Nicotiana alata*). All Arabidopsis experiments used the Col-0 ecotype. Pollen from *N. alata* plants was collected and stored at −80°C until required. Growth medium and culture conditions for *N. alata* pollen were as described by Li et al. (1997).

Phylogenetic Analysis

The phylogenetic tree generated from sequence alignments of AtARAD1-like sequences from *Physcomitrella patens*, *Selaginella moellendorffii*, tomato (*Solanum lycopersicum*), potato (*Solanum tuberosum*), rice (*Oryza sativa*), maize (*Zea mays*), and Arabidopsis was created with the aid of Phylogeny.fr (Dereeper et al., 2008) and visualized using Archaeopteryx (Han and Zmasek, 2009). Briefly, a MUSCLE (Edgar, 2004) multiple sequence alignment with default parameter settings was generated. A Gblock function was used for refinement of the alignment, and a maximum likelihood phylogenetic analysis was performed with the PHYML software tool (Guindon et al., 2005). The nonparametric approximate likelihood-ratio test was used for branch support value as an alternative to bootstrapping (Anisimova and Gascuel, 2006), and branches with values below 0.9 were collapsed.

Molecular Biology

Sequences of primers used in this study are shown in Supplemental Table S2. RNA was isolated from *N. alata* tissues, and first-strand cDNA synthesis was carried out as described previously (Lampugnani et al., 2013a). The *NaARADL1* coding sequence (CDS) was amplified from pollen grain cDNA using primers NaARADL1-01F and NaARADL102R (Supplemental Table S1), sequenced directly, and deposited in the DNA Data Bank of Japan (accession no. LC121596).

RNA in situ hybridization was performed as described previously (Stahle et al., 2009).

The *NaARADL1* promoter was cloned using a nested PCR strategy with 5′ primers designed to the orthologous region in *N. benthamiana* (pNbARADL1-03F) and a 3′ anchor primer, NaARADL1-04R, based on the *NaARADL1* CDS. This ensured that the PCR product would be specific to *NaARADL1*. The resulting PCR product was sequenced directly. To generate pNaARADL1(2.3):GUS, primers pNaARADL1-05F and pNaARADL1-06R were used to amplify an internal fragment for homologous recombination with the reporter GUSplus (Broothaerts et al., 2005) and recombined into the shuttle vector pMIGRO, a derivative of pBJ36 (Lampugnani et al., 2012). The *Not*I expression cassette was then transferred to the binary vector pMLBART (Gleave, 1992) and transformed into the *Agrobacterium tumefaciens* strain AGL1 (Lazo et al., 1991). Plants were transformed by the floral dip method, and transformants were selected for BASTA resistance. Plants were stained for expression of the reporter gene using 2 mM 5-bromo-4-chloro-3-indolyl-β-glucuronic acid and 3 mM $K_3Fe(CN)_6/K_4Fe(CN)_6$ following Lampugnani et al. (2013b). Stained material was observed as whole mounts or as 7- to 8-μm JB-4 plastic (ProSciTech)-embedded sections viewed under light- or dark-field optics. The GUS product is pink under the latter conditions unless very abundant, in which case it appears blue. To ensure that the expression pattern detected is regulated by *NaARADL1* and not due to positional effects (van Leeuwen et al., 2001), 15 independent T1 plants were examined. Only patterns seen consistently in all lines are discussed.

The construct pLAT52:NaARADL1-CERULEAN encodes the fluorescent reporter CERULEAN translationally fused to the C-terminal end of NaARADL1 under the control of the pollen-specific promoter *LAT52* (Twell et al., 1989). To generate this vector, p*LAT52* was cloned into the shuttle vector pMIGRO using primers pLAT52-01F and pLAT52-02R, generating the plasmid pLAT52m. The *NaARADL1* CDS (amplified with the primers NaARADL1-07F and NaARADL1-08R) and mCERULEAN (amplified using the primers UFP-01F and UFP-02R) were joined by overlapping extension PCR using the primers NaARADL1-07F and UFP-02R. The fused product was ligated to pLAT52m using the restriction enzyme sites *Kpn*I and *Bam*HI. The Golgi reporter construct used in transient pollen expression experiments was made by amplifying the α-2,6-SIALYLTRANSFERASE (ST):red fluorescent protein (RFP) coding region (Kim et al., 2001) with the primers ST-01F and RFP-01R and ligating the product to pLAT52m in pMIGRO using the restriction enzymes *Bam*HI and *Xba*I. Transient pollen expression experiments used biolistic bombardment according to the method of Wang and Jiang (2011).

35S:NaARADL1-VENUS was made with the same overlapping extension PCR strategy as for pLAT52:NaARADL1-CERULEAN except that the *VENUS* CDS was amplified instead using primers UFP-01F and UFP-02R and the resulting PCR fragment was ligated into pART7, which already contains the cauliflower mosaic virus 35S promoter and 3′-OCS terminator. The *Not*I expression cassette containing 35S:NaARADL1-VENUS was then transferred to the binary vector pMLBART. The Golgi apparatus and endoplasmic reticulum markers used in this study have been described previously (Wilson et al., 2015).

The previously described GO-PROMTO assay was used to validate the type II membrane protein prediction for NaARADL1 (Søgaard et al., 2012). To improve the signal and the signal-to-noise ratio for BiFC experiments, new reporters were generated using the photostable fluorescent protein VENUS split at amino acid 155 such that the N-terminal version contained the first 155 amino acids (VN155) and the C-terminal version contained the last 84 amino acids (VC155). Amino acid 152 in VENUS was changed from Ile to Leu [VN155(I152L)], as this lowers self-assembly when coexpressed with VC155 and improves the signal-to-noise ratio (Kodama and Hu, 2010). VN155(I152L) and VC155 were synthesized downstream of a 20-amino acid Gly linker and cloned into pFUERTE as described previously (Wilson et al., 2015). The resulting vectors 35S:MCS-gLINKER-V(I152L)N and 35S:MCS-gLINKER-VC were named pURIL and pDOX, respectively (MCS = multiple cloning site). All BiFC constructs used in this study were generated using the primers listed in Supplemental Table S1 and cloned into either an *Sfo*I- and *Kpn*I-linearized pURIL or pDOX. The constructs generated were verified through sequencing and transformed into the AGL1 strain of *A. tumefaciens* by electroporation with the helper plasmid pSOUP, as described previously (Lampugnani et al., 2012).

Transient Expression in *N. benthamiana* Leaves

Transient expression in *N. benthamiana* leaves was carried out as described previously (Lee et al., 2014). Briefly, the abaxial surface of leaves was injected with a mix of *A. tumefaciens* AGL1 strain carrying the BiFC constructs described earlier and another strain generating P19 protein to suppress gene silencing (Voinnet et al., 2003). The final optical density at 600 nm of each *A. tumefaciens* strain was adjusted to 0.8 in infiltration buffer (0.01 M $MgCl_2$ and 0.8 mM acetosyringone) prior to infiltration. After 3 d, leaf sectors were excised, mounted in water, and visualized as described below. Each inoculation was performed on duplicate leaves, and all transformations were performed on at least three separate occasions.

Microscopy

Immunofluorescence and immunoelectron microscopy detection of cell wall polysaccharides was carried out as described previously (Lampugnani et al., 2013a) except that monoclonal antibodies LM13 and LM6 were used (PlantProbes).

Imaging of immunofluorescence was carried out on an inverted Leica SP2 confocal microscope using a 63× PL Apo BL oil objective (numerical aperture 1.4). A 488-nm laser line, attenuated to 20%, was used to excite both Alexa Fluor 488 and FM4-64. Emissions were detected simultaneously between 498 and 530 nm for Alexa Fluor 488 and between 650 and 800 nm for FM4-64. Photodetectors were set at 700, offset by −5. Images were collected using the average of eight optical slices, and z-stacks were taken with successive 0.25-μm scans.

Imaging of fluorescent constructs was carried out using the microscope and lenses described above. A 458-nm laser line, attenuated to 60%, was used to excite mCERULEAN, a 514-nm laser line, attenuated to 50%, was used to excite mVENUS, and a 561-nm laser line, attenuated to 30%, was used to excite mCHERRY. Emissions were detected sequentially between 468 and 504 nm for mCERULEAN, between 524 and 557 nm for mVENUS, and between 571 and 630 for mCHERRY. Photodetectors were set at 700, offset by −5. Images were collected using the average of eight optical slices.

Root Pressure Analysis

Arabidopsis Col-0 and *NaARADL1*-overexpressing plants (12 plants per genotype) were placed into a sealed plastic chamber with their roots in water and their aerial parts open to the atmosphere 26 DAG. The aerial parts were excised by cutting the hypocotyl immediately below the cotyledons and leaves, and positive pressure was applied to the chamber to encourage xylem flow. The volume of sap exuded by the stump was measured for the next 10 min, and the value was expressed on the basis of root dry weight.

Guttation Fluid Collection

Guttation fluid from *NaARADL1*-overexpressing lines was collected using a pipette from the base of rosette leaves of glasshouse-grown plants 26 DAG. To induce guttation in the wild type, plants were transferred to a high-humidity (approximately 75%) growth chamber 4 d prior to collection.

Polysaccharide Compositional Analyses

Cell wall preparations (as alcohol-insoluble residue) and methylation analyses of neutral carbohydrates were as described by Pettolino et al. (2012). For guttation fluid, monosaccharide analyses were performed by either methanolysis (Lea-Smith et al., 2007) or by 2 M trifluoroacetic acid at 100°C for 2 h (Pettolino et al., 2012).

Mass Spectrometry

For the analysis of arabino-oligosaccharides using mass spectrometry, samples were mixed in a 1:1 ratio with matrix containing 1 mg mL^{-1} dihydroxybenzoic acid in 50% (v/v) acetonitrile/0.1% (v/v) trifluroacetic acid and allowed to dry on the polished steel target plate. MALDI-TOF-MS analyses were performed using a MicroFlex MALDI-TOF-MS instrument (Bruker Daltonics). Spectra were acquired using FlexControl software version 3.3 in positive ion reflector mode between *m/z* 600 and 4,000. The parameters were set as follows: ion source 1, 19 kV; ion source 2, 16.3 kV; lens, 9.7 kV; gating, low strength; pulsed ion extraction, 200 ns; detector gain voltage, 1,400 V; electronic gain, enhanced (100-mV offset); sample rate, 2 giga-samples s^{-1}; and laser attenuator offset, 25%. Mass spectrometry data were collected using the following parameters: laser shots, 400 in 20 different positions; and random walk movement. Mass spectrometry data analyses were performed with FlexAnalysis software (version 3; Bruker Daltonics).

To sequence the arabinan polysaccharide in the guttation fluid, the samples were methylated (Pettolino et al., 2012) and analyzed by tandem mass spectrometry using electrospray ionization on a QSTAR Elite hybrid quadrupole time-of-flight mass spectrometer (Applied Biosystems/MDS Sciex). Samples were infused with 50% acetonitrile through an EconoTip (New Objective), with the mass spectrometer operated in the positive ion mode with an ion source voltage of 2,100 V. Analyst QS 2.0 software (Sciex) was used to collect data in the manual mode.

General Methods

The concentration of carbohydrates in the guttation fluid was determined using the colorimetric phenol-sulfuric acid assay (Dubois et al., 1951), and the fluid itself was subjected to CoMPP (Moller et al., 2012) using the arabinan antibodies LM6 and LM13, the XyG antibody LM15, the HG antibody JIM5 (all from PlantProbes), and the AGP antibody JIM16 (CarboSource).

Sequence data from this article can be found in the DDBJ data libraries under accession number LC121596.

Supplemental Data

The following supplemental materials are available.

Supplemental Figure S1. Protein sequence of NaARADL1 and related sequences from Arabidopsis.

Supplemental Figure S2. Gene organization of *NaARADL1*, *At3g45400*, and *AtARAD1*.

Supplemental Figure S3. Expression profile of *NaARADL1* in various *N. alata* tissues.

Supplemental Figure S4. In situ hybridization with probes to *N. alata PHAVOLUTA* and *NaARADL1*.

Supplemental Figure S5. Arabidopsis transgenic plants expressing NaARADL1-VENUS.

Supplemental Figure S6. CoMPP analysis of carbohydrate epitopes present in the guttation fluid from wild-type Arabidopsis and transgenic lines expressing NaARADL1-VENUS.

Supplemental Figure S7. ESI-MS^2 spectrum recorded upon fragmentation of the quasi-molecular ions at *m/z* 1,029 from the endoarabinanase-digested product of the guttation fluid from plants expressing 35S: NaARAT1-VENUS.

Supplemental Table S1. Linkage analysis of sugars in the walls of wild-type and NaARADL1-expressing Arabidopsis lines.

Supplemental Table S2. DNA primers used in this study.

Supplemental Movie S1. Transient NaARADL1-CERULEAN expression in *N. alata* pollen tubes growing in culture.

ACKNOWLEDGMENTS

We thank Prof. Stephen Tyerman (University of Adelaide) and Dr. Sunil Ratnayake (University of Melbourne) for discussions; Cherie Beahan and Roshan Cheetamun for assistance with the carbohydrate linkage analysis; Dr. Sarah Wilson (Australian Research Council Centre of Excellence in Plant Cell Walls, University of Melbourne) for assistance with transmission electron micrography; Kris Ford for assistance with ESI-MS^2 analyses; Prof. Malcolm McConville, Joachim Kloehn, and colleagues (Department of Biochemistry and Molecular Biology and Bio21 Institute, University of Melbourne) for assistance and the provision of instruments used in the methanolysis experiments; and the Biological Optical Microscopy Platform at the University of Melbourne for access to equipment.

Received January 4, 2016; accepted February 4, 2016; published February 5, 2016.

LITERATURE CITED

Anders N, Wilkinson MD, Lovegrove A, Freeman J, Tryfona T, Pellny TK, Weimar T, Mortimer JC, Stott K, Baker JM, et al (2012) Glycosyl transferases in family 61 mediate arabinofuranosyl transfer onto xylan in grasses. Proc Natl Acad Sci USA **109:** 989–993

Anisimova M, Gascuel O (2006) Approximate likelihood-ratio test for branches: a fast, accurate, and powerful alternative. Syst Biol **55:** 539–552

Atmodjo MA, Hao Z, Mohnen D (2013) Evolving views of pectin biosynthesis. Annu Rev Plant Biol **64:** 747–779

Atmodjo MA, Sakuragi Y, Zhu X, Burrell AJ, Mohanty SS, Atwood JA III, Orlando R, Scheller HV, Mohnen D (2011) Galacturonosyltransferase (GAUT)1 and GAUT7 are the core of a plant cell wall pectin biosynthetic homogalacturonan:galacturonosyltransferase complex. Proc Natl Acad Sci USA **108:** 20225–20230

Beveridge T, Wrolstad RE (1997) Haze and cloud in apple juices. Crit Rev Food Sci Nutr **37:** 75–91

Boavida LC, Shuai B, Yu HJ, Pagnussat GC, Sundaresan V, McCormick S (2009) A collection of Ds insertional mutants associated with defects in male gametophyte development and function in Arabidopsis thaliana. Genetics **181:** 1369–1385

Bolwell GP, Northcote DH (1983) Arabinan synthase and xylan synthase activities of Phaseolus vulgaris: subcellular localization and possible mechanism of action. Biochem J **210:** 497–507

Broothaerts W, Mitchell HJ, Weir B, Kaines S, Smith LM, Yang W, Mayer JE, Roa-Rodríguez C, Jefferson RA (2005) Gene transfer to plants by diverse species of bacteria. Nature **433:** 629–633

Brown DM, Zhang Z, Stephens E, Dupree P, Turner SR (2009) Characterization of IRX10 and IRX10-like reveals an essential role in glucuronoxylan biosynthesis in Arabidopsis. Plant J **57:** 732–746

Brownfield L, Ford K, Doblin MS, Newbigin E, Read S, Bacic A (2007) Proteomic and biochemical evidence links the callose synthase in Nicotiana alata pollen tubes to the product of the NaGSL1 gene. Plant J **52:** 147–156

Brownfield L, Wilson S, Newbigin E, Bacic A, Read S (2008) Molecular control of the glucan synthase-like protein NaGSL1 and callose synthesis during growth of Nicotiana alata pollen tubes. Biochem J **414:** 43–52

Cankar K, Kortstee A, Toonen MA, Wolters-Arts M, Houbein R, Mariani C, Ulvskov P, Jorgensen B, Schols HA, Visser RG, et al (2014) Pectic arabinan side chains are essential for pollen cell wall integrity during pollen development. Plant Biotechnol J **12:** 492–502

Cantarel BL, Coutinho PM, Rancurel C, Bernard T, Lombard V, Henrissat B (2009) The Carbohydrate-Active EnZymes database (CAZy): an expert resource for glycogenomics. Nucleic Acids Res **37:** D233–D238

Churms SC, Merrifield EH, Stephen AM, Walwyn DR (1983) An L-arabinan from apple-juice concentrates. Carbohydr Res **113:** 339–344

Cornuault V, Manfield IW, Ralet MC, Knox JP (2014) Epitope detection chromatography: a method to dissect the structural heterogeneity and inter-connections of plant cell-wall matrix glycans. Plant J **78:** 715–722

Dardelle F, Lehner A, Ramdani Y, Bardor M, Lerouge P, Driouich A, Mollet JC (2010) Biochemical and immunocytological characterizations of Arabidopsis pollen tube cell wall. Plant Physiol **153:** 1563–1576

Dardelle F, Le Mauff F, Lehner A, Loutelier-Bourhis C, Bardor M, Rihouey C, Causse M, Lerouge P, Driouich A, Mollet JC (2015) Pollen tube cell walls of wild and domesticated tomatoes contain arabinosylated and fucosylated xyloglucan. Ann Bot (Lond) **115:** 55–66

Dereeper A, Guignon V, Blanc G, Audic S, Buffet S, Chevenet F, Dufayard JF, Guindon S, Lefort V, Lescot M, et al (2008) Phylogeny.fr: robust phylogenetic analysis for the non-specialist. Nucleic Acids Res **36:** W465–W469

Doblin MS, De Melis L, Newbigin E, Bacic A, Read SM (2001) Pollen tubes of *Nicotiana alata* express two genes from different β-glucan synthase families. Plant Physiol **125:** 2040–2052

Domon B, Costello C (1988) A systematic nomenclature for carbohydrate fragmentations in FAB-MS/MS spectra of glycoconjugates. Glycoconj J **5:** 397–409

Dubois M, Gilles K, Hamilton JK, Rebers PA, Smith F (1951) A colorimetric method for the determination of sugars. Nature **168:** 167

Edgar RC (2004) MUSCLE: multiple sequence alignment with high accuracy and high throughput. Nucleic Acids Res **32:** 1792–1797

Esau K (1977) Anatomy of Seed Plants. John Wiley & Sons, Singapore

Ferguson C, Teeri TT, Siika-aho M, Read SM, Bacic A (1998) Location of cellulose and callose in pollen tubes and grains of Nicotiana tabacum. Planta **206:** 452–460

Geshi N, Harholt J, Sakuragi Y, Jensen JK, Scheller HV (2011) Plant polysaccharides, biosynthesis and bioengineering: glycosyltransferases of the GT47 family. Annu Plant Rev **41:** 265–284

Gibeaut DM, Pauly M, Bacic A, Fincher GB (2005) Changes in cell wall polysaccharides in developing barley (Hordeum vulgare) coleoptiles. Planta **221:** 729–738

Gleave AP (1992) A versatile binary vector system with a T-DNA organisational structure conducive to efficient integration of cloned DNA into the plant genome. Plant Mol Biol **20:** 1203–1207

Guindon S, Lethiec F, Duroux P, Gascuel O (2005) PHYML Online: a web server for fast maximum likelihood-based phylogenetic inference. Nucleic Acids Res **33:** W557–W559

Han MV, Zmasek CM (2009) phyloXML: XML for evolutionary biology and comparative genomics. BMC Bioinformatics **10:** 356

Hansen SL, Ray PM, Karlsson AO, Jørgensen B, Borkhardt B, Petersen BL, Ulvskov P (2011) Mechanical properties of plant cell walls probed by relaxation spectra. Plant Physiol **155:** 246–258

Harholt J, Jensen JK, Sørensen SO, Orfila C, Pauly M, Scheller HV (2006) ARABINAN DEFICIENT 1 is a putative arabinosyltransferase involved in biosynthesis of pectic arabinan in Arabidopsis. Plant Physiol **140:** 49–58

Harholt J, Jensen JK, Verhertbruggen Y, Søgaard C, Bernard S, Nafisi M, Poulsen CP, Geshi N, Sakuragi Y, Driouich A, et al (2012) ARAD proteins associated with pectic arabinan biosynthesis form complexes when transiently overexpressed in planta. Planta **236:** 115–128

Heslop-Harrison J (1987) Pollen germination and pollen-tube growth. *In* KL Giles, J Prakash, eds, International Review of Cytology (Pollen: Cytology and Development), **Vol 107**. Academic Press, Orlando, Florida, pp 1–78

Iwai H, Ishii T, Satoh S (2001) Absence of arabinan in the side chains of the pectic polysaccharides strongly associated with cell walls of Nicotiana plumbaginifolia non-organogenic callus with loosely attached constituent cells. Planta **213:** 907–915

Johnson MA, Preuss D (2002) Plotting a course: multiple signals guide pollen tubes to their targets. Dev Cell **2:** 273–281

Jones L, Milne JL, Ashford D, McQueen-Mason SJ (2003) Cell wall arabinan is essential for guard cell function. Proc Natl Acad Sci USA **100:** 11783–11788

Kim DH, Eu YJ, Yoo CM, Kim YW, Pih KT, Jin JB, Kim SJ, Stenmark H, Hwang I (2001) Trafficking of phosphatidylinositol 3-phosphate from the trans-Golgi network to the lumen of the central vacuole in plant cells. Plant Cell **13:** 287–301

Kodama Y, Hu CD (2010) An improved bimolecular fluorescence complementation assay with a high signal-to-noise ratio. Biotechniques **49:** 793–805

Konishi T, Ohnishi-Kameyama M, Funane K, Miyazaki Y, Konishi T, Ishii T (2010) An arginyl residue in rice UDP-arabinopyranose mutase is required for catalytic activity and autoglycosylation. Carbohydr Res **345:** 787–791

Konishi T, Ono H, Ohnishi-Kameyama M, Kaneko S, Ishii T (2006) Identification of a mung bean arabinofuranosyltransferase that transfers arabinofuranosyl residues onto (1, 5)-linked α-L-arabino-oligosaccharides. Plant Physiol **141:** 1098–1105

Lampugnani ER, Kilinc A, Smyth DR (2012) PETAL LOSS is a boundary gene that inhibits growth between developing sepals in Arabidopsis thaliana. Plant J **71:** 724–735

Lampugnani ER, Kilinc A, Smyth DR (2013b) Auxin controls petal initiation in Arabidopsis. Development **140:** 185–194

Lampugnani ER, Moller IE, Cassin A, Jones DF, Koh PL, Ratnayake S, Beahan CT, Wilson SM, Bacic A, Newbigin E (2013a) In vitro grown pollen tubes of Nicotiana alata actively synthesise a fucosylated xyloglucan. PLoS ONE **8:** e77140

Lazo GR, Stein PA, Ludwig RA (1991) A DNA transformation-competent Arabidopsis genomic library in Agrobacterium. Biotechnology (N Y) **9:** 963–967

Lea-Smith DJ, Pyke JS, Tull D, McConville MJ, Coppel RL, Crellin PK (2007) The reductase that catalyzes mycolic motif synthesis is required for efficient attachment of mycolic acids to arabinogalactan. J Biol Chem **282:** 11000–11008

Lee JE, Lampugnani ER, Bacic A, Golz JF (2014) SEUSS and SEUSS-LIKE 2 coordinate auxin distribution and KNOXI activity during embryogenesis. Plant J **80:** 122–135

Li H, Bacic A, Read SM (1997) Activation of pollen tube callose synthase by detergents: evidence for different mechanisms of action. Plant Physiol **114:** 1255–1265

Li H, Bacic A, Read SM (1999) Role of a callose synthase zymogen in regulating wall deposition in pollen tubes of Nicotiana alata Link et Otto. Planta **208:** 528–538

Li X, Cordero I, Caplan J, Mølhøj M, Reiter WD (2004) Molecular analysis of 10 coding regions from Arabidopsis that are homologous to the MUR3 xyloglucan galactosyltransferase. Plant Physiol **134:** 940–950

Lin D, Lopez-Sanchez P, Gidley MJ (2015) Binding of arabinan or galactan during cellulose synthesis is extensive and reversible. Carbohydr Polym **126:** 108–121

Madson M, Dunand C, Li X, Verma R, Vanzin GF, Caplan J, Shoue DA, Carpita NC, Reiter WD (2003) The MUR3 gene of *Arabidopsis* encodes a xyloglucan galactosyltransferase that is evolutionarily related to animal exostosins. Plant Cell **15:** 1662–1670

Mascarenhas JP (1993) Molecular mechanisms of pollen tube growth and differentiation. Plant Cell **5:** 1303–1314

Mohnen D (2008) Pectin structure and biosynthesis. Curr Opin Plant Biol **11:** 266–277

Moller IE, Pettolino FA, Hart C, Lampugnani ER, Willats WG, Bacic A (2012) Glycan profiling of plant cell wall polymers using microarrays. J Vis Exp e4238

Odzuck W, Kauss H (1972) Biosynthesis of pure araban and xylan. Phytochem **11:** 2489–2494

Pagnussat GC, Yu HJ, Ngo QA, Rajani S, Mayalagu S, Johnson CS, Capron A, Xie LF, Ye D, Sundaresan V (2005) Genetic and molecular identification of genes required for female gametophyte development and function in Arabidopsis. Development **132:** 603–614

Peña MJ, Carpita NC (2004) Loss of highly branched arabinans and debranching of rhamnogalacturonan I accompany loss of firm texture and cell separation during prolonged storage of apple. Plant Physiol **135:** 1305–1313

Pettolino FA, Walsh C, Fincher GB, Bacic A (2012) Determining the polysaccharide composition of plant cell walls. Nat Protoc **7:** 1590–1607

Sims IM, Munro SLA, Currie G, Craik D, Bacic A (1996) Structural characterisation of xyloglucan secreted by suspension-cultured cells of Nicotiana plumbaginifolia. Carbohydr Res **293:** 147–172

Søgaard C, Stenbæk A, Bernard S, Hadi M, Driouich A, Scheller HV, Sakuragi Y (2012) GO-PROMTO illuminates protein membrane topologies of glycan biosynthetic enzymes in the Golgi apparatus of living tissues. PLoS ONE **7:** e31324

Stahle MI, Kuehlich J, Staron L, von Arnim AG, Golz JF (2009) YABBYs and the transcriptional corepressors LEUNIG and LEUNIG_HOMOLOG maintain leaf polarity and meristem activity in *Arabidopsis*. Plant Cell **21:** 3105–3118

Takeda F, Wisniewsk ME, Glenn DM (1991) Occlusion of water pores prevents guttation in older strawberry leaves. J Am Soc Hortic Sci **116:** 1122–1125

Talbott LD, Ray PM (1992) Molecular size and separability features of pea cell wall polysaccharides: implications for models of primary wall structure. Plant Physiol **98:** 357–368

Turnbull CG, Lopez-Cobollo RM (2013) Heavy traffic in the fast lane: long-distance signalling by macromolecules. New Phytol **198:** 33–51

Twell D, Wing R, Yamaguchi J, McCormick S (1989) Isolation and expression of an anther-specific gene from tomato. Mol Gen Genet **217:** 240–245

van Leeuwen W, Ruttink T, Borst-Vrenssen AW, van der Plas LH, van der Krol AR (2001) Characterization of position-induced spatial and temporal regulation of transgene promoter activity in plants. J Exp Bot **52:** 949–959

Velasquez SM, Ricardi MM, Dorosz JG, Fernandez PV, Nadra AD, Pol-Fachin L, Egelund J, Gille S, Harholt J, Ciancia M, et al (2011) O-Glycosylated cell wall proteins are essential in root hair growth. Science **332:** 1401–1403

Verhertbruggen Y, Marcus SE, Chen J, Knox JP (2013) Cell wall pectic arabinans influence the mechanical properties of Arabidopsis thaliana inflorescence stems and their response to mechanical stress. Plant Cell Physiol **54:** 1278–1288

Verhertbruggen Y, Marcus SE, Haeger A, Verhoef R, Schols HA, McCleary BV, McKee L, Gilbert HJ, Knox JP (2009) Developmental complexity of arabinan polysaccharides and their processing in plant cell walls. Plant J **59:** 413–425

Voinnet O, Rivas S, Mestre P, Baulcombe D (2003) An enhanced transient expression system in plants based on suppression of gene silencing by the p19 protein of tomato bushy stunt virus. Plant J **33:** 949–956

Wang H, Jiang L (2011) Transient expression and analysis of fluorescent reporter proteins in plant pollen tubes. Nat Protocols **6:** 419–426

Wegner LH (2014) Root pressure and beyond: energetically uphill water transport into xylem vessels? J Exp Bot **65:** 381–393

Willats WGT, Marcus SE, Knox JP (1998) Generation of a monoclonal antibody specific to (1 → 5)-α-L-arabinan. Carbohydr Res **308:** 149–152

Wilson SM, Ho YY, Lampugnani ER, Van de Meene AM, Bain MP, Bacic A, Doblin MS (2015) Determining the subcellular location of synthesis and assembly of the cell wall polysaccharide (1,3;1,4)-β-D-glucan in grasses. Plant Cell **27:** 754–771

Wu AM, Rihouey C, Seveno M, Hörnblad E, Singh SK, Matsunaga T, Ishii T, Lerouge P, Marchant A (2009) The Arabidopsis IRX10 and IRX10-LIKE glycosyltransferases are critical for glucuronoxylan biosynthesis during secondary cell wall formation. Plant J **57:** 718–731

Xu C, Liberatore KL, MacAlister CA, Huang Z, Chu YH, Jiang K, Brooks C, Ogawa-Ohnishi M, Xiong G, Pauly M, et al (2015) A cascade of arabinosyltransferases controls shoot meristem size in tomato. Nat Genet **47:** 784–792

York WS, Kumar Kolli VS, Orlando R, Albersheim P, Darvill AG (1996) The structures of arabinoxyloglucans produced by solanaceous plants. Carbohydr Res **285:** 99–128

Zhong R, Peña MJ, Zhou GK, Nairn CJ, Wood-Jones A, Richardson EA, Morrison WH III, Darvill AG, York WS, Ye ZH (2005) *Arabidopsis fragile fiber8*, which encodes a putative glucuronyltransferase, is essential for normal secondary wall synthesis. Plant Cell **17:** 3390–3408